Received: October 5, 2021 | Accepted: November 7, 2021 | Web Released: December 23, 2021 CL-210619

Hollow Core-satellite ZIF-8/PDA/AgNPs Nanocomplexes: Fabrication, Structure and Antibacterial Activity

Xiaoyi Xu, Qiqi Liu, Shuhan Hui, and Shan Jiang*
Institute of Physical Chemistry, College of Chemistry, Jilin University, Changchun 130012, P. R. China

E-mail: sjiang@jlu.edu.cn

A hollow core-satellite ZIF-8/PDA/AgNPs was established and studied as an antibacterial agent. Polydopamine (PDA) was coated on ZIF-8 surface to form a hollow structure because ZIF-8 core was etched by the chelation of PDA and Zn^{2+}. Then AgNPs were homogeneously decorated on the surface of ZIF-8/PDA by *in situ* reduction of Ag^{+} to avoid their aggregation. ZIF-8/PDA/AgNPs have good antibacterial activity, and they can totally inhibit bacterial growth at the concentration of 16 μg mL^{-1}.

Keywords: ZIF-8 | AgNPs | Antibacterial

Metal-organic frameworks (MOFs) comprise a geometrically unequivocal defined structure with coordination bonds between metal connecting points and organic ligands.[1] Zeolitic imidazolate frameworks-8 (ZIF-8), known as a subclass of MOFs, can be easily prepared by reaction of Zn^{2+} and 2-methylimidazole.[2] Taking advantage of the special properties including high porosity, high loading capacity and easy functionalization, ZIF-8 can be explored for many applications, such as catalysis,[3] chemical sensors,[4] and drug delivery.[5] In particular, Zn^{2+}, an essential element in the body, has good antibacterial capability, thus ZIF-8 has the potential as antimicrobial agent to inhibit bacterial growth.[6]

Silver has been used for centuries as bactericide in medical and consumer products, due to broad-spectrum and strong antimicrobial characteristics.[7] Silver nanoparticles (AgNPs) can continually release silver ions (Ag^{+}) and enable Ag^{+}-induced bacterial inactivation through the disruption of ATP production and DNA replication.[8] However, AgNPs tend to aggregate, causing their antimicrobial activity to be reduced or even completely lost.[9] To solve this problem, researchers have fixed AgNPs onto various carriers including silica,[10] polymers,[11] and carbon nanomaterials[12] to enhance their stability and antibacterial activities.

Dopamine is a neurotransmitter that can adhere to various material surfaces by self-polymerization to form a biocompatible polydopamine (PDA) shell with a large amount of catechol and amine groups.[13] Interestingly, silver nitrate can be *in situ* reduced to AgNPs which well disperse on the surface of a PDA shell layer due to the weak reducibility of PDA shell.[14] Meanwhile, PDA shell can stabilize AgNPs to prevent their aggregation.[15]

In this work, ZIF-8 was firstly coated with PDA shell in virtue of good adhesion ability. ZIF-8/PDA/AgNPs nanocomposites were then prepared by *in situ* reduction of AgNPs with uniform size and good dispersion on the surface of PDA coated ZIF-8. The synthesis of ZIF-8/PDA/AgNPs composites is depicted in Scheme 1. This method successfully prevented the aggregation of AgNPs. Meanwhile, AgNPs and ZIF-8 both have antibacterial activities, which can enhance the synergistic bactericidal effect.

ZIF-8 nanoparticles were synthesized ~250 nm in diameter, when the ratio of 2-methylimidazole and zinc nitrate was 2:1 (Figure 1a). They had uniform morphology and good dispersion. Then a PDA shell with ~26 nm thickness was formed on the surface of ZIF-8 by *in situ* polymerization of dopamine (Figure 1b). ZIF-8/PDA had a similar morphology to ZIF-8, while the bight inner part realized its hollow core-shell structure. PDA shell could fully etch the ZIF-8 core to form a hollow structure due to the chelation of PDA to Zn^{2+}. Zn^{2+} in ZIF-8 is coordinated with the amino groups of PDA and releases 2-methylimidazole.[16] The zeta-potential of ZIF-8/PDA was reduced to −6.2 mV from 42.0 mV of ZIF-8, indicating the successful coating of PDA (Figure 1d). Sequentially, AgNPs were decorated on the surface of ZIF-8/PDA to form ZIF-8/PDA/AgNPs via *in situ* reduction of Ag^{+} by means of the catechol and amine groups of PDA.[17] Transmission electron microscope (TEM) images showed that the AgNPs homogeneously distributed on the surface without obvious aggregation and their size was ~23 nm (Figure 1c). The successful decoration of AgNPs was also proved by the presence of a new peak at 430 nm in the absorption spectra of ZIF-8/PDA/AgNPs (Figure 1e). Finally, the hollow core-satellite nanocomposites were successfully synthesized.

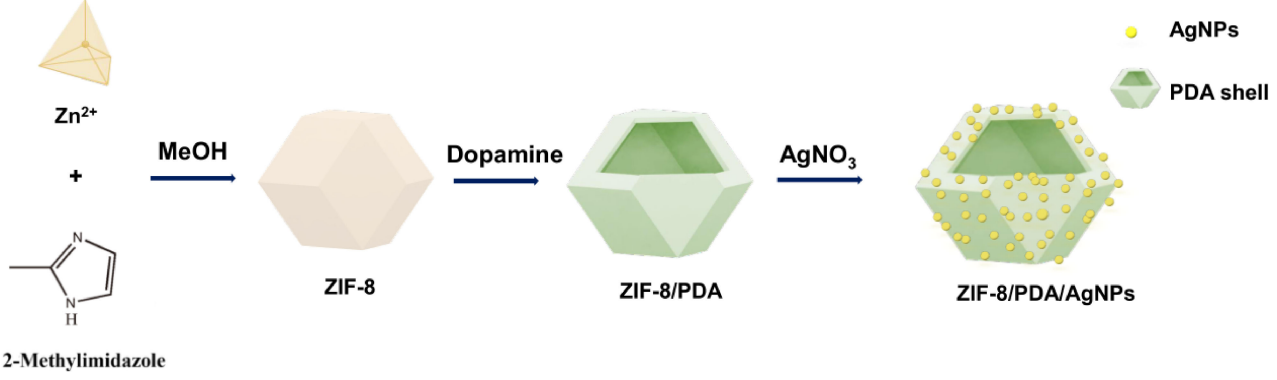

Scheme 1. Schematic illustration of the synthetic procedure for ZIF-8/PDA/AgNPs.

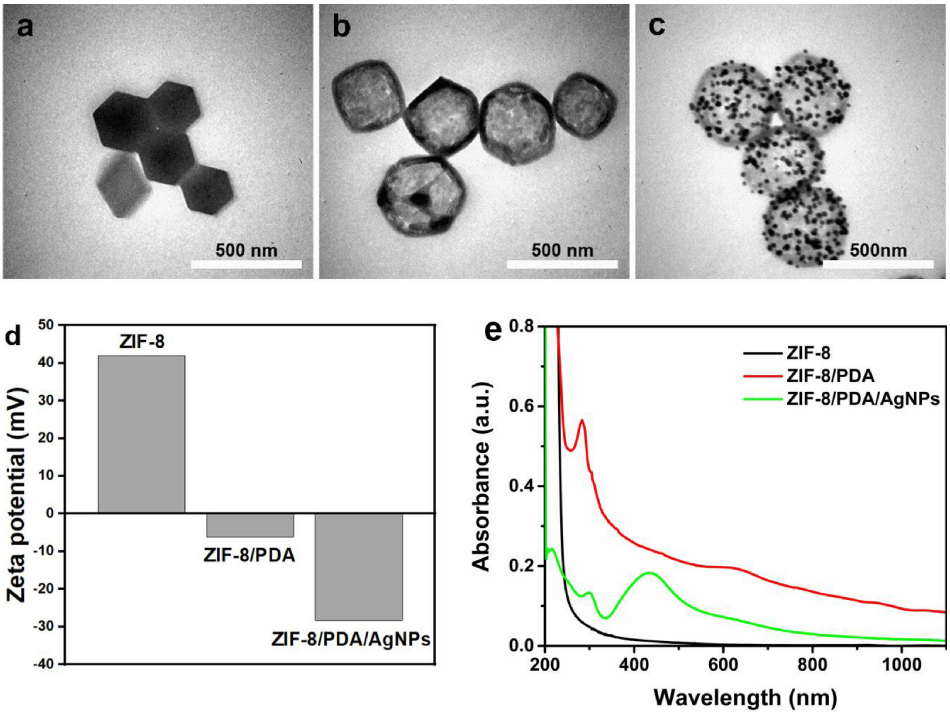

Figure 1. TEM images of (a) ZIF-8, (b) ZIF-8/PDA, and (c) ZIF-8/PDA/AgNPs. (d) Zeta potential and (e) UV-Vis-NIR absorption spectra of ZIF-8, ZIF-8/PDA and ZIF-8/PDA/AgNPs.

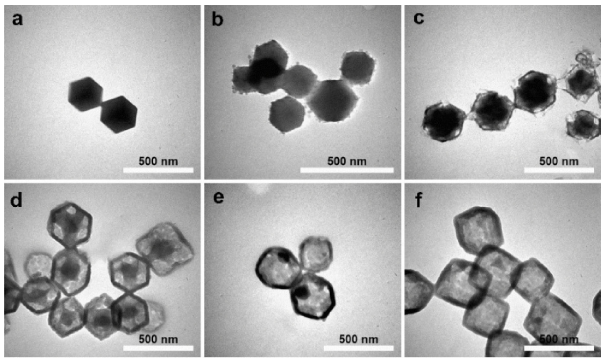

Figure 2. TEM images of ZIF-8/PDA formed at reaction time of (a) 0, (b) 0.5, (c) 1, (d) 3, (e) 5, and (f) 7 h.

The formation process of PDA shell was monitored by using TEM. After reaction of dopamine with ZIF-8 for 30 min, there was a layer of small amorphous particles on the ZIF-8 surface, indicating a small amount of PDA formed at the beginning of the reaction (Figure 2a and 2b). After reaction for 1 h, an incomplete thin layer of PDA formed on the surface of ZIF-8, with a small amount of voids appearing in the core (Figure 2c). After 3 h of reaction, PDA formed a complete shell layer on the surface of ZIF-8, and meanwhile there was a clear gap between the shell and core, establishing a yolk-shell structure (Figure 2d). As the reaction time elapsed, the inner core gradually reduced and the PDA shell gradually became thicker (Figure 2e). At 7 h of reaction, the inner core almost disappeared completely, forming a hollow core-shell structure (Figure 2f). After that, as the reaction time increase, the structure of ZIF-8/PDA remained unchanged. It is considered that the reaction is basically completed after 7 h. During the reaction, ZIF-8 core is gradually etched until it disappears completely along with the formation of PDA shell.

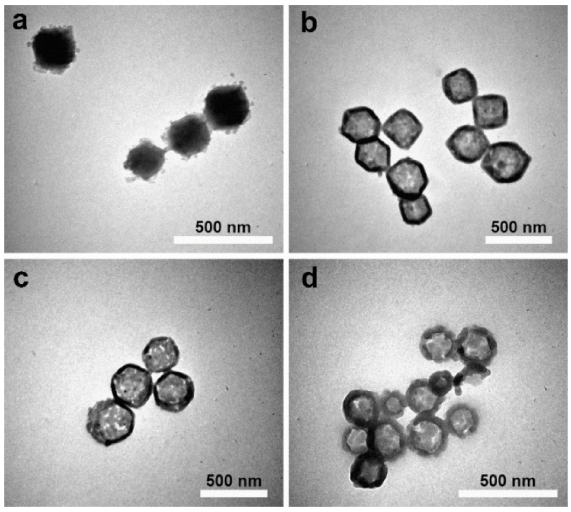

Figure 3. TEM images of ZIF-8/PDA formed at dopamine concentration of (a) 10, (b) 25, (c) 50, and (d) 100 mM.

In order to study the effect of reactant concentration on the morphology and structure of ZIF-8/PDA/AgNPs, different concentrations of dopamine at 10, 25, 50, 100 mM were used for synthesis and observed under TEM. When 10 mM dopamine was added in the ZIF-8 solution and reacted for 7 h, a layer of small amorphous particles grow on the surface of ZIF-8, without forming a complete PDA shell (Figure 3a). Meanwhile, ZIF-8 core was not etched because of the insufficient PDA amount.

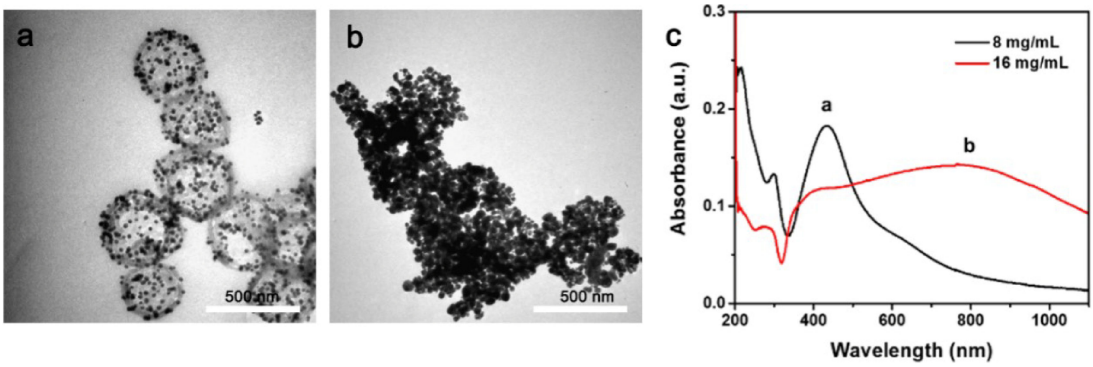

Figure 4. (a, b) TEM images and (c) UV-Vis-NIR absorption spectra of ZIF-8/PDA/AgNPs formed at $AgNO_3$ concentration of (a) 8, (b) 16 mg mL^{-1}.

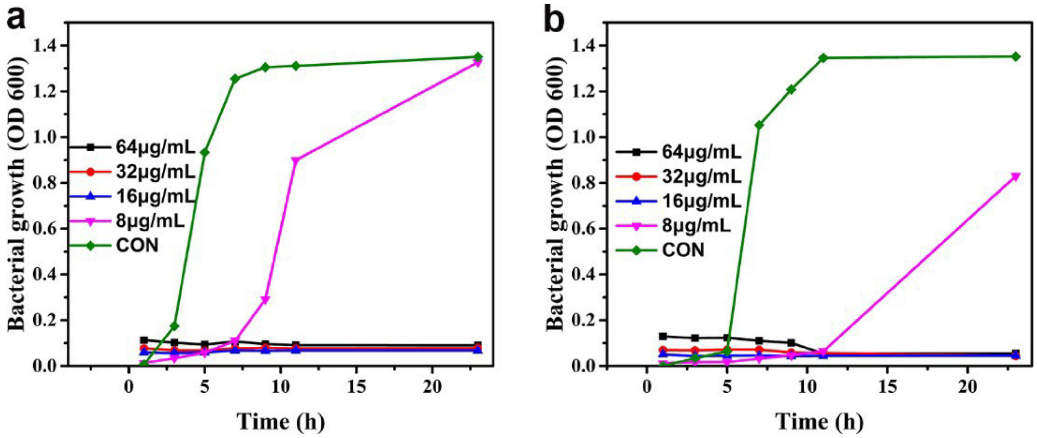

Figure 5. The growth curve of (a) *E. coli* and (b) *S. aureus* bacteria cells. CON is bacterial cells control without any treatment.

When 25 mM was dopamine added, a complete PDA shell was formed on the surface of ZIF-8 with the thickness of 26 nm, and the inner ZIF-8 core was completely etched to form a hollow core-shell structure (Figure 3b). As the concentration of dopamine increased to 50 mM or 100 mM, the thickness of the complete PDA shell increased to 32 nm or 36 nm, and the hollow core-shell structure of ZIF-8/PDA did not change (Figure 3c and 3d). Therefore, ZIF-8/PDA hollow core-shell nanoparticles with different PDA shell thickness can be obtained by adjusting the concentration of dopamine. PDA shell was mainly used for Ag^+ reduction and formation of AgNPs, thus 25 mM dopamine was selected as the reaction condition to form the thin and complete PDA shell.

The concentration of $AgNO_3$ is also one of the important variables to control the morphology of ZIF-8/PDA/AgNPs. After adding 8 mg mL^{-1} $AgNO_3$ to ZIF-8/PDA, a layer of uniform and well-dispersed AgNPs with a size of ~23 nm was formed on the surface (Figure 4a). When the concentration of $AgNO_3$ increased to 16 mg mL^{-1}, the size of AgNPs became larger (~40 nm), and some aggregation of AgNPs appeared (Figure 4b). Meanwhile, the hollow structure of ZIF-8/PDA was destroyed, because excessive $AgNO_3$ can oxidize and degrade the PDA shell.[18] The UV-Vis-NIR absorption spectra of ZIF-8/PDA/AgNPs in Figure 4c was consistent with their TEM results, suggesting 8 mg mL^{-1} of $AgNO_3$ was optimized concentration. In addition, the reaction solvent methanol of ZIF-8/PDA or ZIF-8/PDA/AgNPs was replaced by water. It was found that both hollow ZIF-8/PDA and hollow core-satellite ZIF-8/PDA/AgNPs could not be synthesized possibly because ZIF-8 and ZIF-8/PDA were not stable in water (Figure S1 and S2).

To evaluate the antibacterial ability, we investigated the growth curve of bacteria incubated with ZIF-8/PDA/AgNPs at the concentration of 8, 16, 32, and 64 μg mL^{-1}. The bacterial growth curve represents the number of live cells in a bacterial population over a period of time. In the absence of any treatment, the growth curve of the bacteria showed a slow growth at the beginning, then an exponential growth, and finally reached a stable period in 24 h (Figure 5). When the concentration of ZIF-8/PDA/AgNPs was 8 μg mL^{-1}, the inhibitory effect of bacterial growth appeared in the first 7 h (*E. coli*) or 10 h (*S. aureus*), and then the bacteria gradually started to grow. When the concentration of ZIF-8/PDA/AgNPs increased to 16 μg mL^{-1} or even higher, the growth of both bacteria was totally inhibited within 24 h. The results indicated that 8 μg mL^{-1} ZIF-8/PDA/AgNPs can inhibit bacterial growth within a certain period of time, and 16 μg mL^{-1} nanoparticles can totally inhibit bacterial growth.

To better study the antibacterial mechanism, the morphology of *E. coli* and *S. aureus* exposed to ZIF-8/PDA/AgNPs was investigated by scanning electron microscope (SEM). When

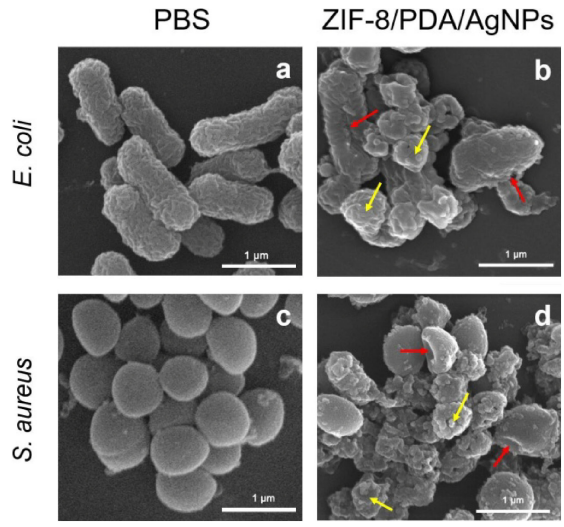

Figure 6. SEM of (a, b) *E. coli* and (c, d) *S. aureus* treated with (a, c) PBS, (b, d) ZIF-8/PDA/AgNPs. The red arrows indicate the damage of bacterial cells. The yellow arrows indicate ZIF-8/PDA/AgNPs.

treated with phosphate buffered saline (PBS), *E. coli* cells were rod-shaped with the intact cell membrane (Figure 6a), and similarly *S. aureus* cells were sphere-shaped with a smooth surface (Figure 6c). When incubated with ZIF-8/PDA/AgNPs, bacterial cells had obvious interaction with nanoparticles, and their cell membrane was damaged, indicating that ZIF-8/PDA/AgNPs have a good bactericidal effect through the interaction with bacterial membrane (Figure 6b and 6d).

In summary, we have prepared ZIF-8/PDA/AgNPs nanoparticles with a hollow core-satellite nanostructure with a size of about 300 nm. The thickness of the PDA shell is 26 nm. The surface is loaded with uniform and well-dispersed AgNPs ~23 nm in size. The effects of different reaction times and the reactant concentration on the morphology and structure of ZIF-8/PDA/AgNPs were investigated. Additionally, the antibacterial properties of ZIF-8/PDA/AgNPs nanoparticles were studied. We found that they have good antibacterial activity against both *E. coli* and *S. aureus*. At 8 μg mL^{-1}, ZIF-8/PDA/AgNPs can inhibit bacterial growth in the initial few hours, while when their concentration increased two-fold, ZIF-8/PDA/AgNPs can totally kill the bacteria.

This work was supported by grants from the National Natural Science Foundation of China (Grant No. 51602123).

Supporting Information is available on https://doi.org/10.1246/cl.210619.

References

1 a) Q. Gao, J. Xu, X.-H. Bu, *Coord. Chem. Rev.* **2019**, *378*, 17. b) O. M. Yaghi, G. Li, H. Li, *Nature* **1995**, *378*, 703.
2 K. S. Park, Z. Ni, A. P. Côté, J. Y. Choi, R. Huang, F. J. Uribe-Romo, H. K. Chae, M. O'Keeffe, O. M. Yaghi, *Proc. Natl. Acad. Sci. U.S.A.* **2006**, *103*, 10186.
3 C. Chizallet, S. Lazare, D. Bazer-Bachi, F. Bonnier, V. Lecocq, E. Soyer, A.-A. Quoineaud, N. Bats, *J. Am. Chem. Soc.* **2010**, *132*, 12365.
4 G. Lu, J. T. Hupp, *J. Am. Chem. Soc.* **2010**, *132*, 7832.
5 H. Zhang, W. Jiang, R. Liu, J. Zhang, D. Zhang, Z. Li, Y. Luan, *ACS Appl. Mater. Inter.* **2017**, *9*, 19687.
6 a) J. Wang, Y. Wang, Y. Zhang, A. Uliana, J. Zhu, J. Liu, B. Van der Bruggen, *ACS Appl. Mater. Interfaces* **2016**, *8*, 25508. b) I. Kohsari, Z. Shariatinia, S. M. Pourmortazavi, *Int. J. Biol. Macromol.* **2016**, *91*, 778.
7 a) Y. Zheng, L. Hou, M. Liu, S. E. Newell, G. Yin, C. Yu, H. Zhang, X. Li, D. Gao, J. Gao, R. Wang, C. Liu, *Sci. Adv.* **2017**, *3*, e1603229. b) G. Franci, A. Falanga, S. Galdiero, L. Palomba, M. Rai, G. Morelli, M. Galdiero, *Molecules* **2015**, *20*, 8856. c) N. von Goetz, L. Fabricius, R. Glaus, V. Weitbrecht, D. Günther, K. Hungerbühler, *Food Addit. Contam.* **2013**, *30*, 612. d) S. Kokura, O. Handa, T. Takagi, T. Ishikawa, Y. Naito, T. Yoshikawa, *Nanomedicine* **2010**, *6*, 570.
8 Y. N. Slavin, J. Asnis, U. O. Hfeli, H. Bach, *J. Nanobiotechnology* **2017**, *15*, 65.
9 A. Panáček, L. Kvítek, R. Prucek, M. Kolář, R. Večeřová, N. Pizúrová, V. K. Sharma, T. Nevěčná, R. Zbořil, *J. Phys. Chem. B* **2006**, *110*, 16248.
10 Z. Deng, M. Chen, L. Wu, *J. Phys. Chem. C* **2007**, *111*, 11692.
11 A. S. Kumbhar, G. Chumanov, *Chem. Mater.* **2009**, *21*, 2835.
12 R. Pasricha, S. Gupta, A. K. Srivastava, *Small* **2009**, *5*, 2253.
13 a) V. K. Thakur, M.-F. Lin, E. J. Tan, P. S. Lee, *J. Mater. Chem.* **2012**, *22*, 5951. b) J. Liebscher, R. Mrówczyński, H. A. Scheidt, C. Filip, N. D. Hădade, R. Turcu, A. Bende, S. Beck, *Langmuir* **2013**, *29*, 10539. c) H. Yang, Y. Lan, W. Zhu, W. Li, D. Xu, J. Cui, D. Shen, G. Li, *J. Mater. Chem.* **2012**, *22*, 16994. d) L. Zhu, Y. Lu, Y. Wang, L. Zhang, W. Wang, *Appl. Surf. Sci.* **2012**, *258*, 5387.
14 a) Y. Zhao, Y. Yeh, R. Liu, J. You, F. Qu, *Solid State Sci.* **2015**, *45*, 9. b) Y. Ma, H. Niu, X. Zhang, Y. Cai, *Analyst* **2011**, *136*, 4192.
15 a) Y. Ma, H. Niu, X. Zhang, Y. Cai, *Chem. Commun.* **2011**, *47*, 12643. b) K. Yoosaf, B. I. Ipe, C. H. Suresh, K. G. Thomas, *J. Phys. Chem. C* **2007**, *111*, 12839.
16 S. Xiang, D. Wang, K. Zhang, W. Liu, C. Wu, Q. Meng, H. Sun, B. Yang, *Chem. Commun.* **2016**, *52*, 10155.
17 Y. Cong, T. Xia, M. Zou, Z. Li, B. Peng, D. Guo, Z. Deng, *J. Mater. Chem. B* **2014**, *2*, 3450.
18 A. Kumar, S. Kumar, W.-K. Rhim, G.-H. Kim, J.-M. Nam, *J. Am. Chem. Soc.* **2014**, *136*, 16317.